Precision Mechanics & Digital Fabrication
https://www.acadlore.com/journals/PMDF

Mathematical Modelling of the Vacuum Degassing Process for Hydrogen Removal in Precision Steel Production

Nenad Milijić[1*], Natalya Safronova[2], Ivan Mihajlović[3*], Aca Jovanović[4]

[1] Engineering Management Department, Technical Faculty in Bor, University of Belgrade, 19210 Bor, Serbia
[2] Department of Organization of Construction and Real Estate Management, Moscow State University of Civil Engineering (National Research University), 26 Moscow, Russia
[3] Industrial Engineering Department, Faculty of Mechanical Engineering, University of Belgrade, 11120 Belgrade, Serbia
[4] Faculty for Project and Innovation Management, Educons University, 11000 Belgrade, Serbia

[*] Correspondence: Nenad Milijić (nmilijic@tfbor.bg.ac.rs); Ivan Mihajlović (imihajlovic@mas.bg.ac.rs)

Received: 10-28-2024 **Revised:** 12-15-2024 **Accepted:** 12-20-2024

Citation: N. Milijić, N. Safranova, I. Mihajlović, and A. Jovanović, "Mathematical modelling of the vacuum degassing process for hydrogen removal in precision steel production," *Precis. Mech. Digit. Fabr.*, vol. 1, no. 4, pp. 216–226, 2024. https://doi.org/10.56578/pmdf010403.

Abstract: Precision steel is a critical material in modern engineering, particularly in precision mechanics and high-performance construction. In this study, a mathematical model is presented to simulate the vacuum degassing (VD) process employed to reduce the hydrogen content in steel produced via the basic oxygen furnace (BOF) process. The steel, which is subsequently used for ingot casting, requires a significant reduction in hydrogen levels— from 7 ppm to below 1.5 ppm—to meet the stringent quality requirements for high-precision applications. This reduction is achieved through the VD process in combination with argon bottom stirring. The model, developed in collaboration with an industrial project in Bosnia and Herzegovina, is designed to predict the necessary degassing time and the temperature variation during the process. The model accounts for the operational parameters specified by the project sponsor and the constraints of the process. Results indicate that the hydrogen content can be reduced within 8.39 minutes under optimal conditions. Furthermore, for a molten steel starting temperature of 1670℃, the final temperature after degassing is predicted to be 1637℃. The applicability of the model has been validated through practical implementation in a new industrial facility, constructed based on the model's predictions. This study demonstrates the broader utility of the model in designing and optimizing VD processes for precision steel production, offering significant potential for enhancing steel quality and process efficiency in similar industrial settings.

Keywords: Precision steel; Precision mechanics; Vacuum degassing (VD); Mathematical modelling

1 Introduction

Precision mechanics, as a contemporary mechanical engineering discipline, requires materials of high purity, which can provide adequate durability and machining properties, in the development of precise tools and products. The technology used should allow for repeatability and accuracy in producing parts. Accordingly, steel materials that will be used for precise mechanics should be in the class standardized as the special steel, stainless steel, or precision steel. Precision steel is a type of steel used in the manufacturing of high-precision products such as aircraft parts, automotive parts, medical devices, and more. For example, the observed development of forging enforces a more and more frequent application of precision forging in closed dies for the production of elements for the automotive industry [1]. This was described in the study conducted by Hawryluk et al. [2], in research related to the assessment of the influence of the impact of the steel grade used for forging punches in terms of the durability of tools used in the precision forging process in closed dies of a chrome-nickel steel valve forging. Also, hardened tool steels have been widely used to make molds and dies by precision milling in aerospace and automotive industries [3]. High-speed precision machining processes have been used in the automotive, aerospace, and tooling industries over the last few decades. To improve a part's surface quality, in particular the surface integrity, and increase the product life cycle are important aspects for these manufacturing industries [4–7]. Accordingly, precision steel fabrication demands great accuracy; e.g., producing steels with advanced properties requires the use of modern steelmaking technologies. A

very important one is degassing, namely the removal of gaseous inclusions such as hydrogen, nitrogen, and oxygen [8]. Degassing is the part of secondary steelmaking. In contemporary steel metallurgy, metals reduction and refining processes almost inevitably involve the controlled interaction of gaseous bubbles in the context of a liquid bath with a gas top space [9]. Accordingly, the hydrogen content for high-quality steel is generally required to be less than 2 ppm [10]. Therefore, during the production of high-quality steel, it is crucial to control the hydrogen content in the molten steel, as excessive hydrogen can lead to issues such as shrinkage, white spots, cracks, and hydrogen embrittlement [10–13], which can subsequently impact the steel's structure and mechanical performance [14]. On the other hand, considering the complexity of the precision steel fabrication, including the degassing processes, numerical analysis, and mathematical modeling, are becoming mandatory stages in the technical development of such techniques [10, 15].

The object of research, described in this paper, was the degassing process of steel, e.g., the hydrogen removal. Hydrogen plays a significant and often different role in the structure and properties of the iron-based alloys [16]. Hydrogen is known as a harmful element causing the hydrogen embrittlement of steel. Hydrogen in steel is in atomic form as an interstitial solid solution with a high speed of diffusion. At defects of the crystal lattice, hydrogen atoms are building molecules. A higher level of dissolved hydrogen can be deleterious for heavy-section products such as pipeline steels, aircraft parts, and ship plate products. For steels with such specific applications, postrefining stir with argon is usually necessary [17]. Accordingly, in modern steel refining procedures, the first and most obvious application of vacuum to extraction metallurgy is to the removal of dissolved gases like hydrogen from molten steel. This, it might appear, could easily be carried out by subjecting a ladle of the melt to low pressure within a vacuum chamber for a short time prior to casting into molds. Unfortunately, the removal of gases under such conditions involves the transport of the gas, as atoms in solution, to the free surface and, particularly, across a diffusion layer at the surface [16, 18]. This makes the process so slow that more elaborate techniques have to be used. Most of the techniques include a combination of the use of a vacuum for gas removal with an inert gas stirring procedure. Namely, the removal of gases from the molten steel can be improved by entering an inert gas such as argon into the stream of metal. This causes a more vigorous sputtering; the argon carries away some of the dissolved gases (as in flushing), and the area exposed is greatly increased with every argon bubble. The argon stirs the metal very effectively and removes dissolved gases. The main disadvantage of this process, when it is applied to steel, is that the temperature falls rather rapidly, making it difficult to reach the teeming bay with the steel still sufficiently hot. The solution to this problem is to start the process with the steel at higher temperatures, which unfortunately would increase the quantity of gas dissolved, which will have to be removed as well as increasing the time available for its removal. Accordingly, it would be of great support to have precise information about the correlation among the time required for degassing and the amount of gases dissolved. So, to be able to decide the temperature of the molten still, at which the degassing procedure should be carried out, it is necessary to facilitate numerical modeling of such systems before practical application. Accordingly, the main topic of this paper was to create a mathematical model that would simulate vacuum gas degassing of steel with argon sputtering, including the modelling of the steel temperature decrease during the procedure. Such a model will give us the data concerning the duration of the degassing process, which should be the input for the calculation of the final steel temperature after degassing. This way, based on the obtained model, the optimal starting temperature of molten steel can be determined for the investigated degassing process.

2 Methodology

The subject of the modelling process, discussed in this paper, was to create a mathematical model that will enable calculation of the time required to complete hydrogen removal from the steel melt. The entire modeling procedure was defined for the purpose of the project: "ICA-01,02,03-001-E: The main project of the ingot casting plant," which was prepared for Arcelor Mittal Steel in Zenica, Bosnia and Herzegovina, which will be denoted as the project sponsor in the remainder of this article. The project proposal was prepared and the entire project realized by the company GLOBEX Group d.o.o. - Engineers and Constructors, registered in Smederevo, Serbia. Authors of this manuscript were the members of the project team and included in all stages of the project preparation and realization in practice.

The boundary conditions for the modeling procedure, presented in this manuscript, were actually indicated as the technological pre-requirements, defined by the project sponsor, and were listed in the project specification, which was part of the tender documentation. This way, the entire numerical model had to be defined based on these boundaries, and the entire metallurgical facility was constructed to fulfill these preset requirements. The initial conditions were: Initial starting hydrogen concentration is 7 ppm, and the final "target" concentration is set to 1.5 ppm. The mass of the steel to be treated in the ladle is 110,000 kg. Carbon content in the steel is C 0.47 mass%; sulfur content in the steel is S 0.020 mass%; phosphorus content in the steel is P 0.012 mass%. Temperature at the beginning of the treatment is 1670°C; temperature at the end of the treatment should be above 1630°C; pre-advanced vacuum in the system will be 250 mbar and advanced vacuum 1 mbar. Based on those predefined conditions, a mathematical model was developed to calculate the time required for the process, and, subsequently, the next step was dealing with determining the temperature decrease during the process. Also, it was required to calculate necessary argon pressure

and its consumption during the process of hydrogen removal.

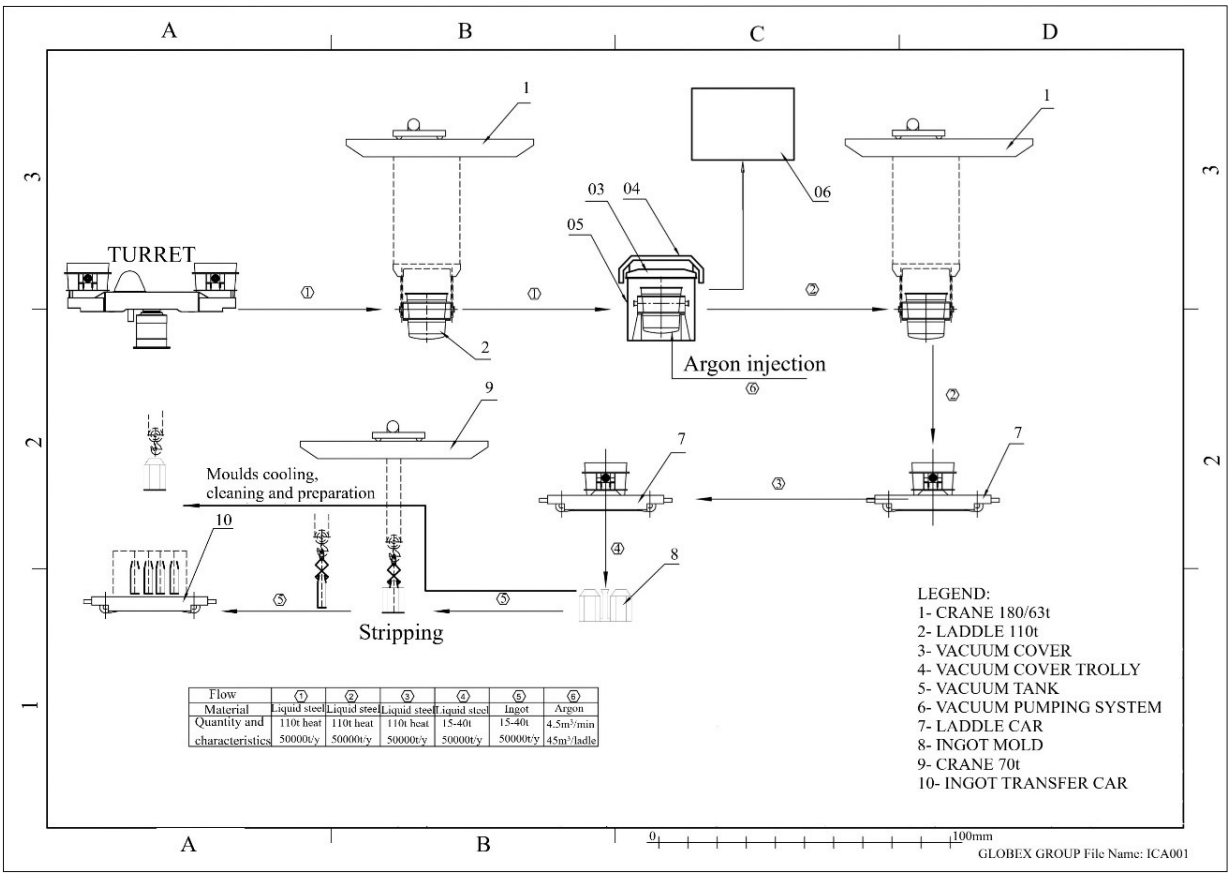

Figure 1. Flow sheet diagram of described degassing process

The technological scheme, containing the mass flow in the process that was used for the final deposition of the equipment during the project implementation phase, is shown in the drawing in Figure 1. Ladle with melted steel (amount of steel is Q = 110 t) is being brought to the location of the vacuum tank (caisson) using the ladle transfer car, from the side of the converter or from the side of the electrical furnace. Ladle is being lifted from the transfer car by a bridge crane with a carrying capacity of Q = 180 t, and the crane transports it to the vacuum tank. Upon the ladle is placed into the vacuum tank, the tank is being closed using the vacuum cover. The cover is being brought and lowered to the tank by a vacuum cover trolley. The vacuum pumping system should be turned on earlier. The vacuum of 250 mbar is obtained in the system using a mechanical vacuum pump running. After the tank is closed, the block valve is opened, and pressure in the system increases rapidly. The mechanical vacuum pump is working and again decreases pressure to 250 mbar. After this level of pressure (vacuum) is reached, the ejector system with steam is being turned on. Absolute pressure achieved by the vacuum system is 1 mbar. Upon finishing the vacuum treatment, the cover is being removed from the tank, and the ladle is relocated onto the ladle car using the crane. Steel quality control before and after the VD procedure is done in the laboratory. The specimen taken from the ladle is being sent to the laboratory via airmail (point-to-point system). Ladle is transferred to the casting pit by the car. Ingot molds are placed into this pit before the transfer of the ladle. Transfer car speed can be regulated, so it is possible to accurately adjust the nozzle of the ladle above the entrance opening of the mold. It is also possible to move the ladle orthogonal to the car trajectory for approximately +/- 100 mm due to adjustment of the nozzle transversally. Transverse travel is performed by hydraulic cylinders that are connected to a hydraulic power unit via a valve stand and fast couplings. After casting and solidification are finished, ingots are taken out (stripping process) by crane with a carrying capacity of 80 MT, and then they are stored for further processing. After the stripping procedure finished, molds are taken out from the casting pit by crane, and the cooling process of the molds starts. When the temperature of the mold is decreased to 100℃, the mold is cleaned and prepared for the new casting operation. Operation of the facility is monitored from the control room and consists of: control cabinet for vacuum facility operating; control cabinet for casting car, including lowering and lifting of the tank cover control; and control cabinet for ladle transfer car control. Control cabinets are placed into the control room. It could be monitored directly or visually via cameras and monitors.

The nucleation of gaseous product is a high order reaction of very high activation energy. The pressure of a small hydrogen bubble is given by [18]:

$$P = 2\sigma/r \tag{1}$$

where, σ is the surface tension of the surrounding melted material, and r is the bubble radius. In molten metal, this pressure is high because the surface tension is high. In steel, $\sigma = 1.6\mathrm{Nm}^{-1}$. The internal pressure in so small a bubble is too high to permit gas molecules to easily enter the initial (nuclei) bubble from surrounding metal with gas in solution at normal industrial concentrations. In the case of hydrogen in steelmaking, the normal range of concentration is 2 ppm to 10 ppm. The appropriate reaction is [16, 18]:

$$\frac{1}{2}\mathrm{H}_2 = \mathrm{H}_{\text{in Fe melt;}} \text{ with Gibbs free energy: } \Delta\mathrm{G}^{\mathrm{O_T}} = 31973 - 44.36 \times \mathrm{T(J)} \tag{2}$$

At 1670℃ (1943 K), there is: $\Delta\mathrm{G}^{\mathrm{O}_{1943}} = 31973 - 44.36 \times 1943 = -54218$ J, with calculated change of the Gibbs free energy, given with Eq. (2):

$$\Delta\mathrm{G}^{\mathrm{O_T}} = -\mathrm{RT}\ln\mathrm{kT} \tag{3}$$

It results with [18]:

ln $\mathrm{k}_{1943} = \frac{-\Delta\mathrm{G}^{\mathrm{O}}_{\mathrm{T}}}{\mathrm{RT}} = \frac{54218}{8.314\times1943} = 3.356$, accordingly, the equilibrium constant k = 28.68. This way: $\mathrm{k} = \frac{\mathrm{H}_{\text{in the Fe melt}}}{\sqrt{p_{\mathrm{H2}}}} = 28.68$ at 1670℃.

Finally, according to the Sievert's law, which states that hydrogen concentration in metals is proportional to the hydrogen partial pressure under thermodynamic equilibrium conditions [16]:

$$\mathrm{H}_{\text{in the Fe melt}} = 28.68 \times \sqrt{\mathrm{p}_{\mathrm{H}_2}} \tag{4}$$

where, $\mathrm{H}_{\text{in the Fe melt}}$ indicates the concentration of dissolved hydrogen in the steel melt, 28.68 is the equilibrium constant, and $\mathrm{p}_{\mathrm{H}_2}$ is the hydrogen partial pressure, leading to: $\mathrm{p}_{\mathrm{H}_2} = \left(\frac{\mathrm{H}_{\text{in Fe melt}}}{28.68}\right)^2$.

The pressure of the gas bubble in the melt is in direct correlation with its dimension, according to the expression given by the Eq. (1). This way, at 1670℃, equilibrium dimensions of stable hydrogen bubbles are presented in Table 1, which was calculated on the basis of Eqs. (1) and (4).

Table 1. Equilibrium dimensions of stable hydrogen bubbles in molten steel

$\mathbf{H}_{\text{in Fe melt}}$ **(ppm)**	$\mathbf{p}_{\mathbf{H}_2}$ **(Pa)**	**Bubble Diameter (m)**
7	6036.072	0.00053
6	4434.665	0.000722
5	3079.628	0.001039
4	1970.962	0.001624
3	1108.666	0.002886
2	492.7406	0.006494
1.5	277.1666	0.011545
1	123.1851	0.025977

Those dimensions present limits above which the creation of stable hydrogen bubbles in Fe melt is possible. Nevertheless, the total resistance toward gas bubble in steel melt is the sum of the pressure of melt atmosphere pa, pressure of metal column p_{Fe} and the tension of bubble formation $2\sigma/\mathbf{r}$ [16, 18]:

$$\mathrm{p}_{\mathrm{total}} = \mathrm{p}_{\mathrm{a}} + \mathrm{p}_{\mathrm{Fe}} + \mathrm{p}_{\mathrm{H}_2} \tag{5}$$

where, $\mathrm{p}_{\mathrm{Fe}} = \rho \times \mathrm{g} \times \mathrm{h}$. Maximal depth of molten steel in the ladle is $\mathrm{h} = 4$ m, and specific gravity of molten steel, at 1670℃, is $\rho = 7160\ \mathrm{kg/m}^3$, leading to: $\mathrm{p}_{\mathrm{Fe}} = \rho \times \mathrm{g} \times \mathrm{h} = 7160 \times 9.81 \times 4 = 280958.4\ \mathrm{Pa} = 2.77\ \mathrm{atm}$. Since the melting pot is under the high vacuum of 1 mBar : $\mathrm{Pa} = 0.000987\ \mathrm{atm}$. This is leading to the total pressure for the steel melt with 7 ppm of hydrogen: $\mathrm{p}_{\mathrm{total}} = 0.000987 + 2.77 + 0.06 = 2.831\ \mathrm{atm}$, with $\mathrm{p}_{\mathrm{H}_2} = 0.06\ \mathrm{atm}$, according to the Table 1.

To become possible for the gas bubble to travel upstream in the steel melt, it is necessary that the inner pressure of the bubble is larger than ptotal. The dimension of such a bubble is: $\mathrm{r} = 2\sigma/\mathrm{P} = 1.11 \times 10^{-5}$ m. The velocity of the

bubble under those conditions can be calculated using Stokes law, which is the mathematical equation that expresses the drag force resisting the fall or upraise of the small spherical particles through a fluid medium [19]:

$$\mathrm{W} = \frac{d^2 \times (\rho_l - \rho_g) \times g}{18 \times \mu}, \quad \mathrm{m/min} \tag{6}$$

where, d is the diameter of the gas bubble dissolved in the melt, ρ_1 is the specific gravity of the molten steel, and ρ_1 is the specific gravity of the dissolved gas; in the form of the bubble, μ is the fluid dynamic viscosity, and g is acceleration due to gravity.

Argon purging in the melt is used for intense agitation of the melt and for the collection of small hydrogen bubbles with much larger argon bubbles. In vacuum ladle degassing, the effectiveness of the degassing process decreases from the top to the bottom of the molten steel bath. Bottom layers of steel are very much less affected by vacuum since these layers are under the influence of ferrostatic pressure due to a column of liquid steel. Hence, bath agitation would help expose the entire content of molten steel to the vacuum. Argon stirring is commonly employed during degassing. Argon bubbling during degassing of molten steel leads to massive volumetric expansion of bubbles due to temperature, because, for example, the volume of gas bubbles becomes 6.3 times higher at 1600°C [20]. Moreover, rising, the inert argon gas bubbles absorb other dissolved gases. Radial expansion of gas bubbles in vacuum processing imparts radial motion to the surrounding fluid [16, 20].

Accordingly, the argon is introduced to the melt with pressure high enough to annulate the pressure of the melts high ($\mathrm{p_{Fe}}$) – e.g., the ferrostatic pressure due to the column of liquid steel, however, the pressure shouldn't be too high because it leads to extensive fizzing of the melt and possible overflow [21]. According to the calculation, the maximal argon pressure for conditions described is 1.5 atm. If the argon is introduced with the pressure of 1.5 atm, the total pressure of the argon bubble at the bottom of the pot would be: $\mathrm{p_{Ar-total}}$ = 0.000987 + 2.77 – 1.5 = 1.274 atm. Based on this value, and in accordance with Eq. (1), the argon bubble radius is much larger than the radius of the hydrogen bubble ($\mathrm{r} = 2\sigma/\mathrm{P} = 2.48 \times 10^{-5}$), leading to its higher velocity according to the Stokes law. The entrance of the hydrogen into the much larger argon bubble could be defined with the same law as the removal of the hydrogen bubble at the surface of the melt, which is already described with Sieverts' law (Eq. (4)).

Based on these considerations, it can be stated that if the concentration of hydrogen in the metal is 7 ppm, the resulting equilibrium partial pressure of hydrogen in the gaseous phase is 0.059571 atm. It would therefore be possible to reduce the hydrogen in the metal below 7 ppm only by reducing the partial pressure of hydrogen below 0.059571 atm. For example, 2 m depth in liquid steel of specific gravity 7160 $\mathrm{kg \cdot \ m^{-3}}$, under vacuum and with introducing argon under pressure of 1 atm, total pressure is $\mathrm{p_{total}} = 0.387\ \mathrm{atm}$. A bubble of argon containing no hydrogen as an impurity would absorb hydrogen to a concentration appropriate to the hydrogen partial pressure of 0.059571 atm. This way $\mathrm{p_{H_2}} = \mathrm{X_{H_2}} \times \mathrm{p_{total,}}$, from which: $0.059571 = \mathrm{X_{H_2}} \times 0.387$, leading to: $\mathrm{X_{H_2}} = 0.154$, and $\mathrm{X_{Ar}} = 1 - 0.154 = 0.846$. Where $\mathrm{X_{H_2}}$ and $\mathrm{X_{Ar}}$ are molar ratios of hydrogen and argon, respectively. Since the bubble travels upwards, at a lesser depth, argon would be tending to absorb new portions of hydrogen since the value of $\mathrm{p_{total}}$ will decrease.

3 Results and Discussion

Mathematical modeling of the VD process was performed using the theoretical framework described in the previous section and based on the predefined industrial conditions—the model boundaries set by the project sponsor. The calculation of the gas bubble diameter was performed based on Eqs. (1)-(5), while the time required for degassing was calculated based on equation 6 and the depth of the molten steel bath, defined by the melting pot. Based on the information that the maximal casting pot depth is 4 meters, for the time calculation, we used a segmental approach. Accordingly, calculation of the time required to lower the hydrogen content in the steel, from 7 ppm to 1.5 ppm, was performed for the segments of 0.1 m of the casting pot height. This way, for different segments that the gas babble has to travel, from the bottom of the melting pot to the surface of the melt, time requirements are presented in Table 2. Results were obtained using the MLAB mathematical software for calculations [22]. MLAB is a tool for mathematical and statistical exploration and for solving simulation and modeling problems such as chemical kinetics, pharmacological compartmental models, ultracentrifuge models, and many more. MLAB is especially designed to handle differential equation models. The modeling in this programming environment, for the case described in this research, was based on the algorithm that was developed based on the Eqs. (1)-(6). The input variables of the model were the melt depth, the starting temperature of the steel, and the initial hydrogen concentration in the melt. Then the algorithm is calculating the ferrostatic pressure of the column of liquid steel at that depth ($\mathrm{P_{Fe}}$), total pressure at that depth of the melt ($\mathrm{P_{total}}$), bubble diameter, velocity of the bubble, and based on the velocity, the time required for the bubble to travel that segment of the melt depth (t). The results in Table 2 are calculated for the initial conditions defined in the case described in this paper [18]; however, the algorithm can also be used for calculations using different depths of the melt, different pressures of argon injection in the melt, and also different starting temperatures of the melted steel.

Table 2. Segmental calculation of the hydrogen removal process duration

Segment	p_{Argon}	Melt Depth	$p_{Fe}(atm)$	$p_{total}\ (atm)$	Bubble Diameter (m)	t (min)
0.1	1.5	4	2.772844	1.273831	2.48E-05	0.990185
0.1	1.5	3.9	2.703523	1.20451	2.62E-05	0.885347
0.1	1.5	3.8	2.634202	1.135189	2.78E-05	0.786373
0.1	1.5	3.7	2.564881	1.065868	2.96E-05	0.693265
0.1	1.5	3.6	2.495559	0.996546	3.17E-05	0.606021
0.1	1.5	3.5	2.426238	0.927225	3.41E-05	0.524642
0.1	1.5	3.4	2.356917	0.857904	3.68E-05	0.449128
0.1	1.5	3.3	2.287596	0.788583	4E-05	0.379479
0.1	1.5	3.2	2.218275	0.719262	4.39E-05	0.315695
0.1	1.5	3.1	2.148954	0.649941	4.86E-05	0.257775
0.1	1.5	3	2.079633	0.58062	5.44E-05	0.20572
0.1	1.5	2.9	2.010312	0.511299	6.18E-05	0.15953
0.1	1.5	2.8	1.940991	0.441978	7.15E-05	0.119205
0.1	1.5	2.7	1.87167	0.372657	8.47E-05	0.084744
0.1	1.5	2.6	1.802348	0.303335	0.000104	0.056149
0.1	1.5	2.5	1.733027	0.234014	0.000135	0.033418
0.1	1.5	2.4	1.663706	0.164693	0.000192	0.016552
0.1	1.5	2.3	1.594385	0.095372	0.000331	0.005551
0.1	1.5	2.2	1.525064	0.026051	0.001212	0.000414
0.1	1	2.1	1.455743	0.45673	6.91E-05	0.127295
0.1	1	2	1.386422	0.387409	8.15E-05	0.091587
0.1	1	1.9	1.317101	0.318088	9.93E-05	0.061743
0.1	1	1.8	1.24778	0.248767	0.000127	0.037764
0.1	1	1.7	1.178459	0.179446	0.000176	0.01965
0.1	1	1.6	1.109138	0.110125	0.000287	0.0074
0.1	1	1.5	1.039816	0.040803	0.000774	0.001016
0.1	0.5	1.4	0.970495	0.471482	6.7E-05	0.135651
0.1	0.5	1.3	0.901174	0.402161	7.85E-05	0.098695
0.1	0.5	1.2	0.831853	0.33284	9.49E-05	0.067603
0.1	0.5	1.1	0.762532	0.263519	0.00012	0.042376
0.1	(0) Argon Blowing Stops	1	0.693211	0.694198	4.55E-05	0.294076
0.1	0	0.9	0.62389	0.624877	5.05E-05	0.238277
0.1	0	0.8	0.554569	0.555556	5.68E-05	0.188342
0.1	0	0.7	0.485248	0.486235	6.5E-05	0.144273
0.1	0	0.6	0.415927	0.416914	7.58E-05	0.106068
0.1	0	0.5	0.346605	0.347592	9.09E-05	0.073728
0.1	0	0.4	0.277284	0.278271	0.000113	0.047253
0.1	0	0.3	0.207963	0.20895	0.000151	0.026643
0.1	0	0.2	0.138642	0.139629	0.000226	0.011897
0.1	0	0.1	0.069321	0.070308	0.000449	0.003017
					Total Time, min	8.393545

Based on the calculations presented in Table 2, it can be noticed that, for the segment between 2 m and 1 m below the surface of the ladle, argon pressure of 1.5 atm would lead to overflow, considering that the p_{Argon} would be above the pressure of the ferrostatic pressure of the column of liquid steel at that depth (p_{Fe}), which is 1.455743 atm at 2.1 meter depth. Accordingly, after 6.56 minutes (when the argon bubble introduced to the bottom of the pot has reached the segment of 2.1 meters below the surface), argon pressure should be lowered down to 1 atm. After the next 20 seconds, it should be lowered again to 0.5 atm, and finally, after the next 20 seconds, it should be completely stopped. Bubbles would travel the rest of their way to the surface under the pressure they already obtained, rapidly enough. This way, the total time required to remove the hydrogen from the steel melt, with argon stirring, is 8.39 min.

Based on the calculations presented in Table 2, argon should be pumped in the melt only for the first 7.26 minutes with the pressure below 1.5 atm. During the remaining time, hydrogen will be removed without further argon introduction. The mechanism of hydrogen absorption, using the argon bubbles, is presented in Figure 2. This figure presents the modeled conditions for the hydrogen removal on different one-meter segments of the melt. Considering that at the deepest segment of the melt (from the bottom of the ladle to the 3-meter depth), the ferrostatic pressure of the melt is highest, which results in the smallest diameters of the hydrogen and argon bubbles and, accordingly, the smallest velocity of their movement. This results in the longest time required for the argon and hydrogen transfer through this segment, equal to 6.09 minutes. In the segment from 3 to 2 meters, below the surface, the r_{H2} and r_{Ar}

diameters increase, leading to an increase of W_{Ar} and W_{H2} that results in a rapid decrease of the required time for the gas bubbles to travel through this segment. The same trend remains for the following segments, closer to the surface, as given in Figure 2.

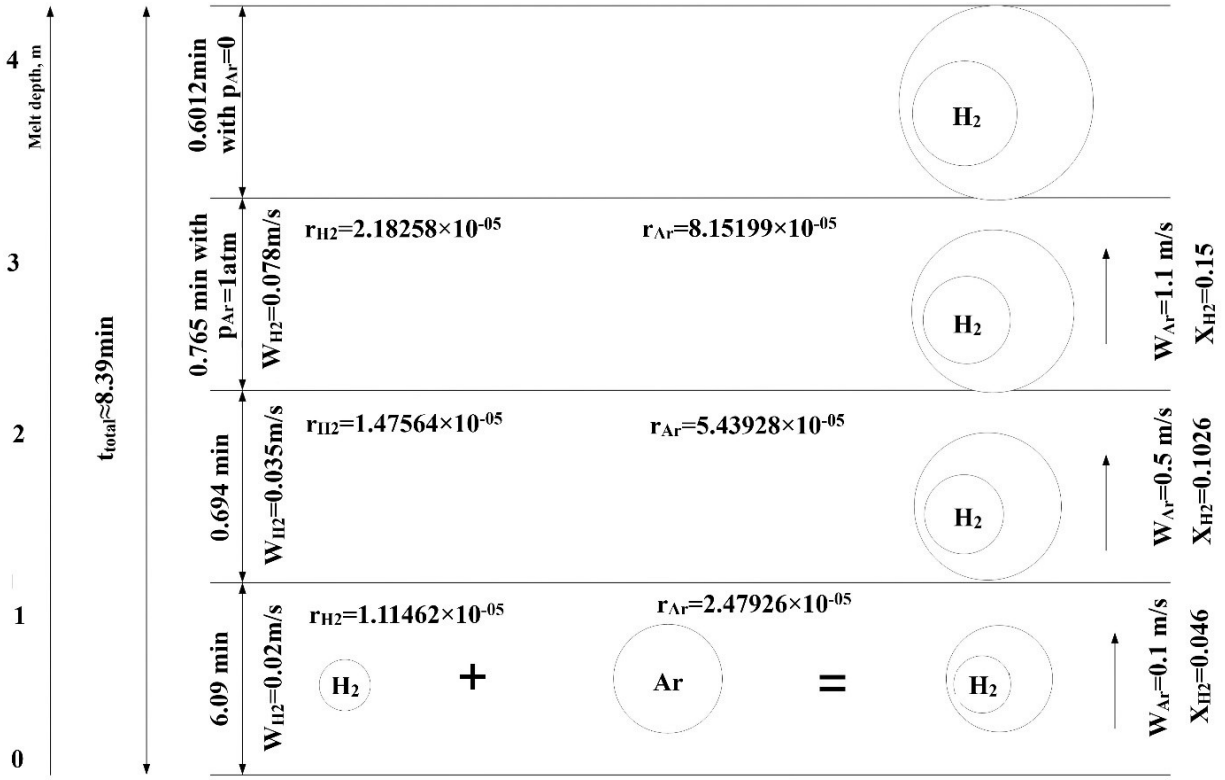

Figure 2. Mechanism of hydrogen removal using the argon bubbles stirring

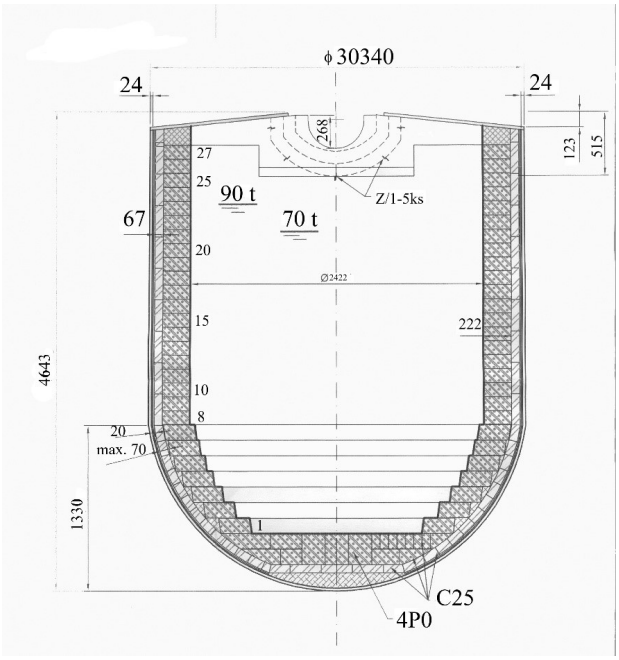

Figure 3. Dimension of the melting pot

3.1 Cooling of Steel Melt During the Period of Degassing

Since the subsequent operation of degassing is casting (Figure 1), an important parameter is the temperature of the steel melt after degassing. To calculate the temperature decrease during degassing, it is necessary to know the amount of argon required for the process, as well as the geometry of the melting pot (presented in Figure 3). If taken into consideration, the molar mass ratio of H_2 and Ar, and after conversion of molar to weight percent, having in mind that the amount of H_2 should be lowered from 7 to 1.5 ppm, for 110 tons of steel, the required amount of argon gas is 4.5 $\mathrm{m} \times \mathrm{min}^{-1}$ (Figure 1). This amount of argon is in the acceptable range according to literature [23, 24]. The equation that can be used to calculate the heat that will be carried out with the gas stream, in such conditions, can be calculated using the equation:

$$Q_{gas} = m \times Cp \times \Delta T \tag{7}$$

The temperature of gas streams, in this kind of system, is in the range 600℃ to 800℃ [8]. Heat carried with argon gas stream (with the heat capacity of argon being $\mathrm{Cp} = 524\ \mathrm{J} \cdot\ \mathrm{kg}^{-1}$) [24] is: $\mathrm{Q_{Ar}} = 32697600$ J. Heat loss with a hydrogen gas stream (with the heat capacity of hydrogen being $\mathrm{Cp} = 14304\ \mathrm{J} \cdot\ \mathrm{kg}^{-1}$ [25]) is: $\mathrm{Q_{H_2}} = 6750000$ J.

3.2 Heat Losses Through the Walls of the Vessel

For the melting pot with maximal dimensions presented in Figure 3, and 110, 000 kg of melt, the inner heat transfer surface (melt-refractory lining) is: $\mathrm{S_1} = 30.42\ \mathrm{m}^2$. Average thickness of the refractory lining is 285 mm. Center heat transfer surface (refractory lining - vessel wall) is $\mathrm{S_2} = 37.58\ \mathrm{m}^2$, and the outside heat transfer surface (vessel wall - air) is $\mathrm{S_3} = 38.18\ \mathrm{m}^2$.

The mechanism of heat exchange is as follows: (a) from the central section of the melt toward the inner lining of magnesite bricks (convective heat transfer), (b) conductive transfer through the lining, (c) conductive transfer through the vessel wall, and (d) convection from the outside surface to the surrounding air. The amount of heat that metal releases according to the above mechanism is: $\mathrm{Q_{tot}} = \frac{\Delta T}{R_t}$, where, R_t is the total heat transfer resistance of the melting pot layers, e.g.:

$$R_t = \frac{1}{\alpha_1 \times S_1} + \frac{\log \frac{r_2}{r_1}}{2 \times \pi \times L \times \lambda_1} + \frac{\log \frac{r_3}{r_2}}{2 \times \pi \times L \times \lambda_2} + \frac{1}{\alpha_2 \times S_3} \tag{8}$$

(a) Since the metal melt is resting in the pot, this should be considered unforced convection, and the equation that could describe this process is

$$Gr = \frac{g \times l^3 \times \beta \times \Delta t}{v^2}$$

where,

- Grash of number: Gr is a dimensionless number that approximates the ratio of the buoyancy to viscous forces acting on a fluid;
- Temperature of the melt: T = 1943 K;
- Coefficient of thermal expansion: $\beta = 5.15 \times 10^{-4}\ \mathrm{K}^{-1}$;
- Kinematic viscosity of steel is $\mu = 0.0057\ \mathrm{kg} \cdot\ \mathrm{m}^{-1} \cdot\ \mathrm{s}^{-1}$ [26], leading to dynamic viscosity of $v = 7.961 \times 10^{-7}\ \mathrm{N} \cdot\ \mathrm{s} \cdot\ \mathrm{m}^{-2}$;
- Specific heat of molten steel is $\mathrm{C_p} = 970\ \mathrm{J} \cdot\ \mathrm{kg}^{-1} \cdot\ \mathrm{K}^{-1}$ [27];
- Coefficient of heat conduction $-\lambda = 20\Omega \cdot \mu^{-1} \cdot\ \mathrm{K}^{-1}$ [18];
- Prandtl number is then: $Pr = \frac{C_p \times \mu}{\lambda} = \frac{970 \times 0.0057}{20} = 0.27645$;

From which: $\mathrm{Gr} = 290.8 \times 10^{12}$ and accordingly $\mathrm{Ra} = \mathrm{Gr} \times \mathrm{Pr} = 290.8 \times 10^{12} \times 0.27645 = 80.39 \times 10^{12}$, leading to $\mathrm{Nu} = 0.13 \times (\mathrm{Ra})^{1/2} = 0.13 \times \left(80.39 \times 10^{12}\right)^{1/3} = 5610.66$.

This way, the coefficient of heat transfer from steel to inner surface of the pot is: $\alpha_1 = \frac{Nu \times \lambda}{l} = \frac{5610.66 \times 20}{4} = 28053.31\ \mathrm{W} \cdot\ \mathrm{m}^{-2}\ \mathrm{K}^{-1}$.

(b) Heat conduction coefficient of magnesite lining brick at operational temperature is $\lambda_1 = 7.42\ \mathrm{W} \cdot\ \mathrm{m}^{-1} \cdot\ \mathrm{K}^{-1}$.

(c) Heat conduction coefficient of vessel wall at operational temperature is $\lambda_2 = 45.46\ \mathrm{W} \cdot\ \mathrm{m}^{-1} \cdot\ \mathrm{K}^{-1}$.

(d) Physical characteristics of the air surrounding the vessel are:

$$\lambda = 2.59 \times 10^{-2}\ \mathrm{W} \cdot\ \mathrm{m}^{-1} \cdot\ \mathrm{K}^{-1}$$
$$\nu = 15.06 \times 10^{-7}\ \mathrm{m}^2 \cdot\ \mathrm{s}^{-1}$$
$$Pr = 0.703$$
$$\beta = 1/293 = 0.0034$$

Resulting with: $\mathrm{Gr} = 545 \times 10^{12}; \mathrm{Ra} = 384 \times 10^{12}$ and $\mathrm{Nu} = 9447$. Accordingly: $\alpha_2 = \frac{Nu \times \lambda}{l} = \frac{9447 \times 2.59 \times 10^{-2}}{4} = 61.17\ \mathrm{W} \cdot\ \mathrm{m}^{-2}\ \mathrm{K}^{-1}$.

From above calculations: $\mathrm{R_t} = 9.27 \times 10^{-4}\ \mathrm{K} \cdot\ \mathrm{W}^{-1}$ and $\mathrm{Q_{tot}} = 1768718.92\ \mathrm{J} \cdot\ \mathrm{s}^{-1}$.

For the time period including 4 minutes for closing the vessel, 10 minutes to drop down the pressure from 100 mbar to 1 mbar , and 8.39 minutes for VD at the pressure of $1\mathrm{mbar}$ (22.39 minutes in total): $\mathrm{Q_{tot}}$ (time)=2376096997.1 J.

3.3 Heat Loss from the Surface Radiation of the Melt

Heat loss from the radiation of the steel surface is happening when the surface of molten steel is opened (4 min) and during the time period of 10 minutes when pressure is decreasing linearly from 1000 to 1 mbar. Heat radiation from the open surface of molten steel could be described with the Stefan-Boltzmann law [28]:

$$\mathrm{Q_{r1}} = \mathrm{C_o} \times \mathrm{S_a} \times \left[\left(\frac{T_1}{100} \right)^4 - \left(\frac{T_2}{100} \right)^4 \right] \times \mathrm{t} \tag{9}$$

where, $\mathrm{C}_o = 5.67\ \mathrm{W} \cdot\ \mathrm{m}^{-2}\ \mathrm{K}^{-1}$ is the Stefan Boltzmann constant; $\mathrm{T_1}$= 1670℃ – temperature of molten steel; $\mathrm{T_2} = 30$℃ – temperature of surrounding air; $\mathrm{t} = 240\ \mathrm{s}; \mathrm{S_a} = 4.6\ \mathrm{m}^2$ – upper surface of the molten steel. Then: $\mathrm{Q_{r1}}$=486347985.60 J.

Heat radiation from the surface of molten steel, during the period of linear pressure drop in the vessel atmosphere (10 min), should be considered using the differential form of Eq. (9):

$$\frac{\partial Q}{\partial t} = \frac{\partial \varepsilon}{\partial t} \times \mathrm{C_o} \times \mathrm{S_a} \times \left[\left(\frac{T_1}{100} \right)^4 - \left(\frac{T_2}{100} \right)^4 \right] \tag{10}$$

where, ε is the coefficient of heat radiation, which changes from 1 to 0, when pressure drops from 1000 mbar (which is the pressure before the vacuum pump is turned on - e.g., the atmospheric pressure) to 1 mbar , which is the pressure of the advanced vacuum in the system, as predefined by the project sponsor. For such conditions in the system, the change of the coefficient of heat radiation, $\frac{\partial \varepsilon}{\partial t}$ is behaving according to the linear scheme presented in Figure 4.

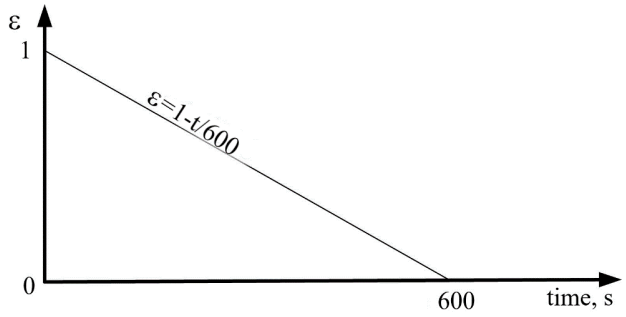

Figure 4. Change of coefficient of heat radiation as the function of time

Accordingly, based on Eq. (10), there are:

$$\frac{\partial Q}{\partial t} = (1 - \mathrm{t}/600) \times \mathrm{C_o} \times \mathrm{S_a} \times \left[\left(\frac{T_1}{100} \right)^4 - \left(\frac{T_2}{100} \right)^4 \right]$$

or

$$\mathrm{Q_{r2}} = \int_{t=0}^{t=600} (1 - \mathrm{t}/600) \times \mathrm{C_o} \times \mathrm{S_a} \times \left[\left(\frac{T_1}{100} \right)^4 - \left(\frac{T_2}{100} \right)^4 \right] \partial t = 607934982.20\ \mathrm{J}.$$

3.4 Overall Heat Loss

According to defined partial heat losses, the overall heat loss is: $\mathrm{Q_{sum}} = \mathrm{Q_{Ar}} + \mathrm{QH_{H2}} + \mathrm{Q_{tot}} + \mathrm{Q_{r1}} + \mathrm{Q_{r2}} = 32697600 + 6750000 + 2376096997 + 486347985 + 607934982 = 3509827564$ J.

This amount of heat loss will lead to the following decrease in molten steel temperature (with heat capacity of steel $\mathrm{C_{ps}} = 970\ \mathrm{J/kgK}$): $3509827564 = 110000 \times 970 \times (1670 - \mathrm{T_2})$. This way, $\mathrm{T_2}$=1637℃, meaning that steel will be cooled for 33℃ during the process of degassing. The cooling of 33℃, may seem too high; however, considering

the amount of steel and the intensity of the process, it can be considered below the acceptable frame of the industry average. Namely, in the reference [8], the temperature drop of 80℃ is reported, with the temperature at the end of the degassing process equal to 1570-1590℃. Also, in the reference [10], it is stated that the effect of steel temperature drop of 50℃ in the industrial VD is assumed to be minor and usually accepted in the model. In the model described in this manuscript, which was also practically proven in the described case in the ingot casting plant in Zenica (Bosnia and Herzegovina), the temperature drop didn't affect any of the subsequent operations in the process, presented in Figure 1.

4 Conclusions

The results presented herein describe a critical stage in the production of high-purity steel, specifically intended for use in precision mechanics. A key aspect of such material production is the development of a mathematical model for the VD process. This model enables the calculation of the time required for degassing, which was determined to be 8.39 minutes under the defined initial conditions. The duration of the VD process is essential for estimating the temperature decrease of molten steel during degassing. Given that the steel will subsequently be cast into ingots, knowledge of the steel's temperature at the commencement of casting is crucial. Under the specified conditions, the temperature of the molten steel after degassing was calculated to be 1637℃, which is sufficient for successful casting.

The model presented in this study served as the foundation for a practical industrial project, resulting in the construction of an ingot casting plant. As such, its practical applicability in real industrial settings cannot be overlooked. The analysis conducted in this study was based on actual data from cast house operations, which ensures that the modeling approach is grounded in real-world conditions. Consequently, the model and the methods described herein can be utilized to design new VD processes or optimize existing ones. These results are applicable to other practitioners, enabling similar calculations under their own predefined conditions.

Furthermore, the reduction of hydrogen content from an initial value of 7 ppm to a final value of 1.5 ppm facilitates the production of steel with superior purity. This, in turn, reduces the embrittlement of the steel and enhances its mechanical properties and machinability.

Nevertheless, the research presented in this manuscript is subject to certain limitations. The focus was primarily on the specific conditions defined by the project sponsor. Future investigations will extend these calculations to include varying initial conditions, such as different starting temperatures and geometries of the melting pots. This will allow for a more comprehensive understanding of how the starting temperature of the molten steel influences the time requirements and temperature decrease during the process. The aim will be to finalize the definition of optimal process conditions, ensuring further refinement of the VD process in future industrial applications.

Data Availability

The data used to support the research findings are available from the corresponding author upon request.

Conflicts of Interest

The authors declare no conflict of interest.

References

[1] Z. Gronostajski and M. Hawryluk, "The main aspects of precision forging," *Arch. Civ. Mech. Eng.*, vol. 8, no. 2, pp. 39–55, 2008. https://doi.org/10.1016/S1644-9665(12)60192-7

[2] M. Hawryluk, M. Lachowicz, M. Zwierzchowski, M. Janik, Z. Gronostajski, and J. Filipiak, "Influence of the grade of hot work tool steels and its microstructural features on the durability of punches used in the closed die precision forging of valve forgings made of nickel-chrome steel," *Wear*, vol. 528–529, p. 204963, 2023. https://doi.org/10.1016/j.wear.2023.204963

[3] A. Reimer and X. C. Luo, "Prediction of residual stress in precision milling of AISI H13 steel," *Procedia CIRP*, vol. 71, pp. 329–334, 2018. https://doi.org/10.1016/j.procir.2018.05.036

[4] I. S. Jawahir, E. Brinksmeier, R. M'Saoubi, D. K. Aspinwall, J. C. Outeiro, D. Meyer, D. Umbrello, and A. D. Jayal, "Surface integrity in material removal processes: Recent advances," *CIRP Ann.*, vol. 60, no. 2, pp. 603–626, 2011. https://doi.org/10.1016/j.cirp.2011.05.002

[5] D. Umbrello, G. Ambrogio, L. Filice, and R. Shivpuri, "A hybrid finite element method–artificial neural network approach for predicting residual stresses and the optimal cutting conditions during hard turning of AISI 52100 bearing steel," *Mater. Des.*, vol. 29, no. 4, pp. 873–883, 2008. https://doi.org/10.1016/j.matdes.2007.03.004

[6] A. Reimer, S. Fitzpatrick, and X. Luo, "A full factorial numerical investigation and validation of precision end milling process for hardened tool steel," in *17th Euspen International Conference & Exhibition*, Hannover, Germany, 2017.

[7] A. Reimer, S. Fitzpatrick, X. C. Luo, and J. Zhao, "Numerical investigation of mechanical induced stress during precision end milling hardened tool steel," *Solid State Phenom.*, vol. 261, pp. 362–369, 2017. https://doi.org/10.4028/www.scientific.net/SSP.261.362

[8] M. Nicolae, C. Predescu, I. Vilciu, M. Sohaciu, and A. Nicolae, "Kinetics of gas removal from steel smelts with advanced characteristics," *J. Optoelectron. Adv. Mater.*, vol. 9, no. 12, pp. 3889–3892, 2007.

[9] W. Cheng, C. L. Fu, and Z. Qian, "Two regularization methods for a spherically symmetric inverse heat conduction problem," *Appl. Math. Model.*, vol. 32, no. 4, pp. 432–442, 2008. https://doi.org/10.1016/j.apm.2006.12.012

[10] J. Zhong, J. Xu, D. Luo, S. Liu, Z. Zhou, and C. Lai, "Numerical simulation on dehydrogenation behavior during argon blowing enhanced vacuum refining process of high-quality steel," *J. Mater. Res. Technol.*, vol. 33, pp. 6481–6493, 2024. https://doi.org/10.1016/j.jmrt.2024.11.034

[11] M. A. Mohtadi-Bonab and M. Masoumi, "Different aspects of hydrogen diffusion behavior in pipeline steel," *J. Mater. Res. Technol.*, vol. 24, pp. 4762–4783, 2023. https://doi.org/10.1016/j.jmrt.2023.04.026

[12] L. Wan, W. T. Geng, A. Ishii, J. P. Du, Q. S. Mei, N. Ishikawa, H. Kimizuka, and S. Ogata, "Hydrogen embrittlement controlled by reaction of dislocation with grain boundary in alpha-iron," *Int. J. Plast.*, vol. 112, pp. 206–219, 2019. https://doi.org/10.1016/j.ijplas.2018.08.013

[13] M. L. Martin and P. Sofronis, "Hydrogen-induced cracking and blistering in steels: A review," *J. Nat. Gas Sci. Eng.*, vol. 101, p. 104547, 2022. https://doi.org/10.1016/j.jngse.2022.104547

[14] U. S. Meda, N. Bhat, A. Pandey, K. N. Subramanya, and M. L. A. Raj, "Challenges associated with hydrogen storage systems due to the hydrogen embrittlement of high strength steels," *Int. J. Hydrogen Energy*, vol. 48, no. 47, pp. 17 894–17 913, 2023. https://doi.org/10.1016/j.ijhydene.2023.01.292

[15] J. Weller, D. Roesmann, S. Eggert, S. von Enzberg, I. Gräßler, and R. Dumitrescu, "Identification and prediction of standard times in machining for precision steel tubes through the usage of data analytics," *Procedia CIRP*, vol. 119, pp. 514–520, 2023. https://doi.org/10.1016/j.procir.2023.01.011

[16] J. D. Gilchrist, *Extraction Metallurgy*. Pergamon Press: New York, NY, USA, 1989.

[17] "Volume 1: Properties and selection: Irons, steels, and high performance alloys," in *ASM Handbook*. ASM International, 1990.

[18] I. Mihajlović, N. Štrbac, L. Balanović, Z. Živković, and A. Jovanović, "Numerical modelling of the vacuum degassing process of molten steel with advanced characteristics," *Optoelectron. Adv. Mater. Rapid Commun.*, vol. 4, no. 3, pp. 385–389, 2010.

[19] S. Moran, *An Applied Guide to Water and Effluent Treatment Plant Design*. Butterworth-Heinemann: UK, 2018. https://doi.org/10.1016/C2016-0-01092-6

[20] "Module 3: Ladle Metallurgy; Lecture 25: Principles of degassing," NPTEL. https://archive.nptel.ac.in/content/storage2/courses/113104059/lecture25/25_6.htm

[21] C. Pfeiler, M. Wu, and A. Ludwig, "Influence of argon gas bubbles and non-metallic inclusions on the flow behavior in steel continuous casting," *Mater. Sci. Eng. A*, vol. 413-414, pp. 115–120, 2005. https://doi.org/10.1016/j.msea.2005.08.178

[22] "MLAB mathematical modeling system," Civilised Software, Inc., MD, USA. https://www.civilized.com

[23] S. E. Malkov, I. Y. Zinurov, and A. M. Shumakov, "Modern small-capacity unit for the vacuum-oxygen refining of steel," *Metallurgist*, vol. 50, pp. 525–528, 2006. https://doi.org/10.1007/s11015-006-0116-4

[24] S. Yamamoto and M. Yoshii, "Method for refining a molten steel in vacuum," Patent U.S. Patent 4,071,356, 1978. https://patents.google.com/patent/US4071356A/en

[25] Z. Meijie, G. Huazhi, H. Ao, Z. Hongxi, and D. Chengji, "Numerical simulation and industrial practice of inclusion removal from molten steel by gas bottom-blowing in continuous casting tundish," *J. Min. Metall. Sect. B-Metall.*, vol. 47, no. 2, pp. 137–147, 2011. https://doi.org/10.2298/JMMB11012006M

[26] Z. Živkovic and V. Savović, *Theory of Pyrometallurgical Processes*. Tehnički Fakultet: Serbia, 1994. https://plus.cobiss.net/cobiss/sr/sr/bib/ubsm/9432847

[27] Y. Miki, Y. Shimada, B. G. Thomas, and A. Denissov, "Model of inclusion removal during RH degassing of steel," *Iron and Steelmaker*, vol. 24, no. 8, pp. 31–38, 1997.

[28] Z. Radovic and M. Lalovic, "Numerical simulation of steel ingot solidification process," *J. Mater. Process. Technol.*, vol. 160, no. 2, pp. 156–259, 2005. https://doi.org/10.1016/j.jmatprotec.2004.07.094